O.O. GAVRYLYUK,[1] O.YU. SEMCHUK,[1] O.V. STEBLOVA,[2] A.A. EVTUKH,[2]
L.L. FEDORENKO [2]

[1] Chuiko Institute of Surface Chemistry, Nat. Acad. of Sci. of Ukraine
 (17, General Naumov Str., Kyiv 03164, Ukraine; e-mail: oleksandr_gavrylyuk@mail.ru)
[2] V. Lashkaryov Institute of Semiconductor Physics, Nat. Acad. of Sci. of Ukraine
 (41, Nauky Ave., Kyiv 03028, Ukraine)

STUDY OF THE DISTRIBUTION
OF TEMPERATURE PROFILES IN NONSTOICHIOMETRIC
SiO$_x$ FILMS AT LASER ANNEALING

The distribution of temperature profiles in nonstoichiometric SiO$_x$ films at the single pulse laser annealing has been studied theoretically. Temperature distributions on the surface of the SiO$_x$ films at irradiation by a laser beam with various intensities have been calculated. Temperature distributions on various depths of the SiO$_x$ films at irradiation by a laser beam with an intensity of 52 MW/cm^2 have been found. During the laser pulse of 10 ns with an intensity of 52 MW/cm^2, the temperature up to 1800 K can be reached on the specimen surface.

K e y w o r d s: SiO$_x$ films, thermal conductivity, nanocrystals.

1. Introduction

The important material of modern microelectronics is silicon (Si). Its electronic and physico-chemical properties have defined the main path of development and the current state of the element base of microelectronics and its technology. Saving Si as the main basic material of microelectronics would be a positive phenomenon, especially because the achievements of planar technology accumulated for more than half a century would be used. One of the most efficient solutions to the problem of preservation of Si as the main material of the future of electronics is its nanostructuring, which includes also the formation of Si nanocrystals in a wide bandgap oxide matrix. The structures of silicon nanoparticles of silicon (nc-Si-nanocrystalline silicon) grown in SiO$_2$ have attracted the attention of researchers due to perspectives in the creation of new functional devices of nanoelectronics. The development of the technology of silicon nanocrystals and nanocomposite SiO$_x$ films, which contain silicon nanocrystals in a dielectric matrix, is the important actual problem of nanoelectronics.

The relatively larger amount of silicon than it is necessary for stoichiometric SiO$_2$ phases can cause the formation of Si-nanoparticles from excess Si atoms.

The migration speed of Si atoms in the dielectric matrix significantly affects the formation of a boundary state between Si nanoparticles and SiO$_2$, allowing the formation of multiple insertions of individual Si atoms in the SiO$_2$ matrix [1]. The thermal annealing of SiO$_x$ films leads to the formation of nanoparticles of different chemical compositions, namely with excess silicon in the film [2]. The formation of the silicon phase is accompanied by the restoration of the stoichiometry of the surrounding oxide matrix. The annealing temperature determines the structure of nanoparticles [3]. The diffusion-limited growth of amorphous Si inclusions begins at 800 °C. At higher annealing temperatures, the growth of particles is accompanied by the crystallization. At the same time, the crystalline Si phase is very unstable, and stable Si nanocrystals are formed only at 1100 °C, which is consistent with the assumption of a strong dependence of the crystallization temperature on the size of the Si inclusion [4]. At the annealing during 1 min at a temperature of 1250 °C, the complete decomposition of the SiO$_x$ phase into Si and SiO$_2$ is realized.

The high-temperature annealing in a furnace (above 1000 °C) is the necessary process for the formation of nc-Si in SiO$_x$. Nevertheless, the processing of a SiO$_x$ film with the typical thermal annealing is not a localized process and can lead during the annealing to the destruction of components of the electronic circuits that are on the same substrate. Rather recently,

the laser annealing began to be used for the formation of nc-Si in SiO_x films [5].

For the efficient use of nanostructures in silicon electronics, it is necessary to perform the comprehensive theoretical and experimental study of the laser annealing process of nonstoichiometric SiO_x films. In this paper, we have carried out the theoretical study of the temperature distribution profiles in nonstoichiometric SiO_x films during the laser annealing process. As a test specimen, the SiO_x film 138 nm in thickness and with the stoichiometry index equal to 0.8 has been used.

2. Theory

The process of heat transfer in solids is the process of heat energy transfer. It is obviously that it is primarily determined by the equation of energy conservation. Let us suppose that $dQ = \rho T dS$ (Q is the amount of heat, which enters the unit volume of the material, ρ is the material density, T is the absolute temperature, and S is the entropy per unit mass of the material). If $dQ = 0$, then the process of heat transfer occurs adiabatically. Adiabatic conditions can be expressed by the equation

$$\frac{dQ}{dt} = \rho T \frac{dS}{dt} = 0. \qquad (1)$$

Let us suppose that $\mathbf{q}$ is the density of the energy flux that is transferred by conduction, then the differential representation of the energy conservation law has the form [1]

$$\rho T \frac{dS}{dt} = -\operatorname{div}\mathbf{q} + \left(\frac{\partial Q}{\partial t}\right). \qquad (2)$$

Equation (2) is the continuity equation for the amount of heat. The adiabatic property of the process is disrupted in the presence of external heat sources (in particular, optical ones), as well as at the consideration of irreversible processes in the system such as thermal conductivity.

In order to obtain the equation describing a change in the ambient temperature from Eq. (2), we make the following assumption. First, we will assume that the change of thermodynamic quantities occurs at a constant pressure [6]

$$T\frac{\partial S}{\partial t} = c_{\mathrm{p}}\frac{\partial T}{\partial t}, \qquad (3)$$

where c_{p} is the specific heat at constant pressure. Second, using the first term of the expansion of the vector $\mathbf{q}$ in degrees of the temperature gradient, we obtain

$$\mathbf{q} = -\kappa \operatorname{grad} T, \qquad (4)$$

where κ is the thermal conductivity coefficient.

If we neglect the temperature dependence of ρ, c_{p}, κ, $\left(\frac{\partial Q}{\partial t}\right)$, then the temperature field spreading on the solid state surface heated by laser radiation can be described by a differential equation of the parabolic type (Fourier equation) [7]

$$\frac{\partial T}{\partial t} = \chi\left(\frac{\partial^2 T}{\partial x^2} + \frac{\partial^2 T}{\partial y^2} + \frac{\partial^2 T}{\partial z^2}\right) + \frac{1}{\rho c_p}\left(\frac{\partial Q}{\partial t}\right), \qquad (5)$$

where $\chi = \frac{\kappa}{\rho c_{\mathrm{p}}}$ is the temperature conductivity, and T is the absolute temperature of the specimen.

Let a laser beam propagate along the OZ axis and fall onto the surface (x, y) of a solid, by creating the volume heat source with a power density of $\left(\frac{\partial Q}{\partial t}\right) = \alpha J(\mathbf{r}, t)$ ($J(\mathbf{r}, t)$ is the intensity distribution of laser radiation in the medium, and α is the laser irradiation absorption coefficient by the surface). For the simplest case of a beam with the Gaussian distribution of the intensity, the equation is [6]

$$J(\mathbf{r}, t) = J_0(1 - R)\exp(-\alpha z) \times$$
$$\times \exp\left\{-\frac{x^2 + y^2}{s^2}\right\} f\left(\frac{t}{\tau_{\mathrm{p}}}\right), \qquad (6)$$

where J_0 is the intensity of laser radiation that is incident on the solid surface, R is the reflecting property of the surface, and s is the radius of the Gaussian beam. The function $f(\frac{t}{\tau_{\mathrm{p}}})$ describes the time dependence of a laser pulse with the duration τ_{p}. For the simulation of a pulsed laser heating of substances, the function $f(\frac{t}{\tau_{\mathrm{p}}})$ is specified with the use of the Heaviside function $\theta(t)$ [6]:

$$f\left(\frac{t}{\tau_{\mathrm{p}}}\right) = \frac{\theta(t) - \theta(t - \tau_{\mathrm{p}})}{\tau_{\mathrm{p}}}. \qquad (7)$$

For finding the temperature distribution on the surface of solids, Eq. (5) can be rewritten in the following form [6–9]:

$$\frac{\partial T}{\partial t} = \chi\left(\frac{\partial^2 T}{\partial x^2} + \frac{\partial^2 T}{\partial y^2} + \frac{\partial^2 T}{\partial z^2}\right) + \frac{\alpha}{\rho c_{\mathrm{p}}} J(x, y, z, t). \qquad (8)$$

The temperature distribution must satisfy the following boundary and initial conditions. Because of the periodicity of problems, the sources and the heat flows must converge to zero at the borders of the periodic structure. Then we can write

$$\frac{\partial T}{\partial x}\Big|_{x=\pm a} = 0, \quad \frac{\partial T}{\partial y}\Big|_{y=\pm b} = 0. \tag{9}$$

On the surface $z = 0$, the heat flow is absent:

$$\frac{\partial T}{\partial z}\Big|_{z=0} = 0. \tag{10}$$

Thus, it is necessary to consider that

$$\lim_{t \to 0} T = 0. \tag{11}$$

We also accept the zero initial conditions for the temperature:

$$T(x, y, z, 0) = 0. \tag{12}$$

A solution of the above-formulated problem can be constructed by using Green's functions [10, 11]. However, the nontrivial task of calculating the improper integrals arises in this approach. So, we choose another way. We note that Eq. (8) has constant coefficients and is homogeneous. In this case, the variables are separated in the source function. Under such circumstances, the method of integral transforms [12] can be convenient.

While solving the problem of determination of the spatial and time distributions of the surface temperature of solids under laser heating, we use the finite integral transformation in the (x, y) coordinates and the cosine Fourier transformation in the z coordinate [7, 8, 13]. The consistent implementation of these transformations (regardless of their order) leads to a family of inhomogeneous ordinary differential equations of the first order in time. After their solution and the transition in the original space, we obtain the solution of problem (8)–(11) as the convergent series and the integral.

To simulate the temperature profile in the corresponding film, the following laser pulse parameters have been used: a pulse duration of 10 ns, and the laser beam intensities in the interval 14–52 MW/cm^2.

The distribution of the temperature field in the SiO$_x$ film heated by a single laser pulse is described by Eq. (5). For the problem under consideration, it can be rewritten as follows [14, 15]:

$$\rho c_{\mathrm{p}} \frac{\partial T}{\partial t} - \nabla[k(T)\nabla T] = \alpha I_0(t)(1 - R)\exp(-\alpha y), \tag{13}$$

where $\alpha = \frac{2\omega n_1}{c} = \frac{4\pi n_2}{\lambda} = \frac{1}{\delta}$, I_0 is the intensity of a single laser pulse, $k(T)$ is the thermal conductivity coefficient, τ is the laser pulse duration, λ is the laser radiation wavelength, n_1 is the refractive index, n_2 is the extinction coefficient, c is the speed of light, ω is the circular frequency, and δ is the penetration depth.

The boundary conditions on the top and bottom surfaces of the specimen are described by the equation

$$-n\,q = h\,(T - T_{\mathrm{amb}}) + \sigma\sigma_{\mathrm{SB}}\left(T^4 - T_{\mathrm{amb}}^4\right), \tag{14}$$

where σ is the coefficient of surface emission, $\sigma_{\mathrm{SB}} = 5.67 \times 10^{-8}$ is the Stefan–Boltzmann constant, n is the normal vector, h is the heat transfer coefficient, and T_{amb} is the ambient temperature. The heat flow from the laser irradiation is included in the model as a volume source. For the definite description of the energy flow, it is necessary to specify the nature of a pulse laser emission in the Gaussian form,

$$I_0(t) = \frac{F_0}{\tau}\exp\left\{-\frac{4(t - \tau)^2}{\tau^2}\right\}, \tag{15}$$

where F_0 is the flux density of laser radiation.

The symmetric thermal insulation conditions on the vertical surfaces of the specimen are given as

$$\frac{\partial T}{\partial n} = 0. \tag{16}$$

Initial conditions are chosen as

$$T = T_{\mathrm{amb}}. \tag{17}$$

Thus, the system of equations (13)–(17) describes the process of pulse laser annealing of the SiO$_x$ films.

The equation of heat conduction (13) is solved by the numerical finite element method.

3. Results and Discussion

The calculated temperature distributions on the SiO$_x$ film surface irradiated by laser beams with different intensities are shown in Fig. 1.
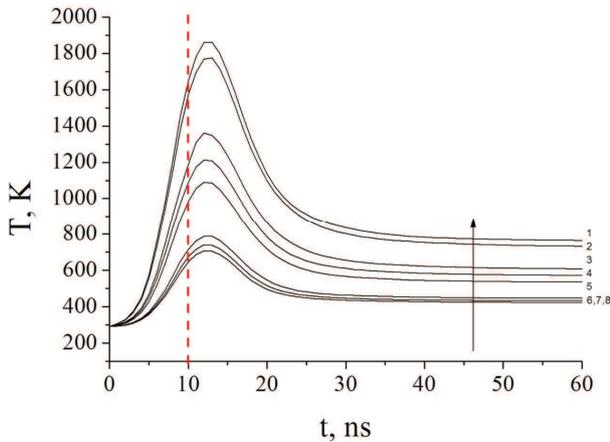
Fig. 1. Specimen surface temperature calculated by Eq. (13) versus the laser pulse duration for various intensities of irradiation: *1* – 52 MW/cm^2; *2* – 49 MW/cm^2; *3* – 35 MW/cm^2; *4* – 31 MW/cm^2; *5* – 27 MW/cm^2; *6* – 17.2 MW/cm^2; *7* – 15.7 MW/cm^2; *8* – 14.7 MW/cm^2

Fig. 2. Dependences of the calculated surface temperature of the specimen at the center of a laser beam on the intensity of laser radiation at different times after the beginning of annealing

Fig. 3. Dependences of the calculated surface temperature of the specimen on the x coordinate with the time as a parameter: *1* – t = 1 ns, *2* – 10 ns, *3* – 20 ns, *4* – 30 ns, *5* – 80 ns. Laser pulse intensity is 52 MW/cm^2

As can be seen from Fig. 1, the temperature at the surface grows for some time after the laser pulse ($\tau = 10$ ns) finished. The further cooling of the film is due to the flow of heat from the film surface and also due to the heat transfer into the silicon substrate. After 30 ns from the beginning of the irradiation, the annealing temperature on the surface of the film is stabilized. The stabilized temperature depends on the laser intensity: the higher the intensity, the higher is the temperature. The temperatures of the specimen at higher intensities of laser irradiation are enough to stimulate the phase transition of SiO$_x$ film into a nanocomposite SiO$_2$(Si) film with Si nanocrystals [16]. But it is not clear which time is sufficient for the phase separation. It was shown in [17] that, at the temperatures of 1200 and 1350 °C, the Si nanocrystals were formed during 1 s and 20 ms, respectively. The investigation of the laser annealing of nanocrystalline films performed in argon [18] showed that single and multiple laser pulses improve the crystalline structure of the films. The high-power single-pulse annealing can easily damage the film, but the low energy density multiple pulse irradiation can result in the annealing without damage [18].

As shown in Fig. 2, the dependences of the surface temperature of the specimen on the laser radiation intensity at different times have the linear behavior.
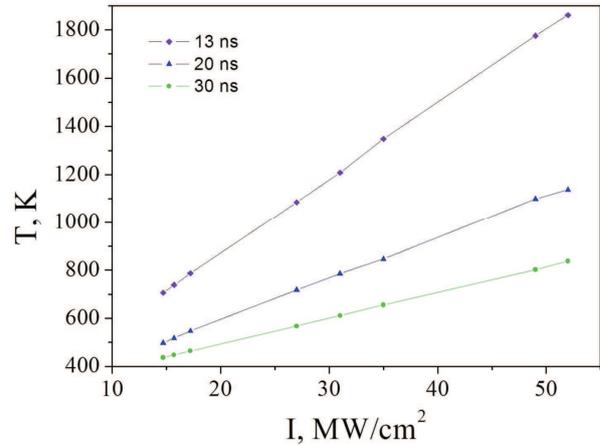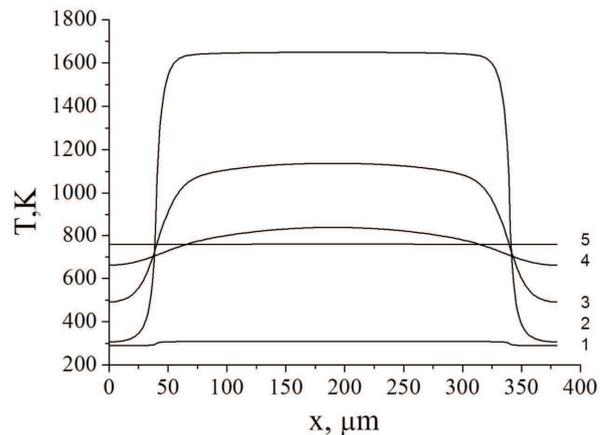
This makes it possible to predict the temperature at the surface with increase in the laser radiation intensity in certain intervals.

The temperature distribution along the x coordinate on the surface of the specimen is shown in Fig. 3. As can be expected, the maximum surface temperature decreases with time, and the temperature profile changes its shape. Instead of a sharp drop of the temperature outside the laser beam, there is the smooth flow of heat to the periphery and into the interior of the specimen (Figs. 3 and 4). As a result, the volume
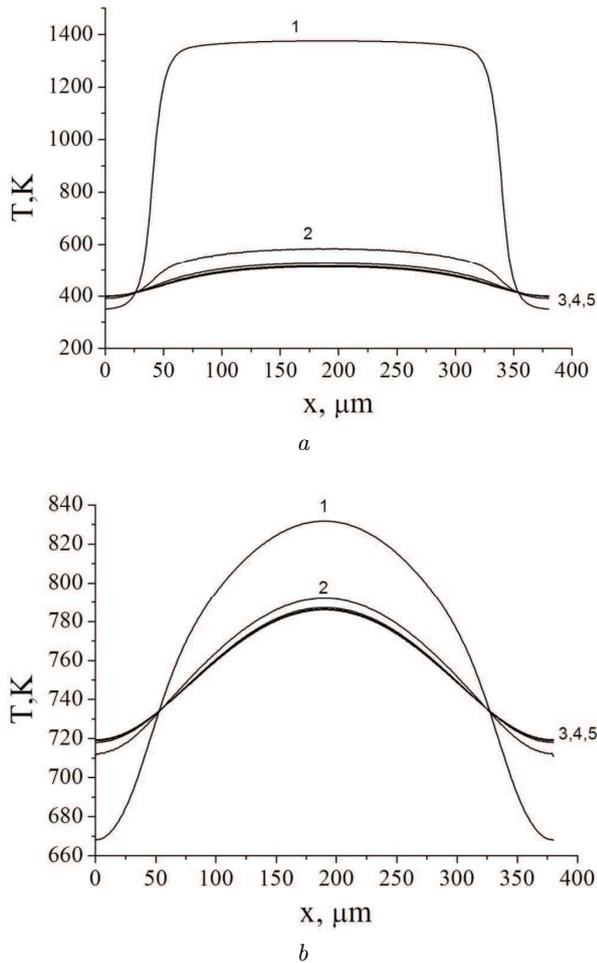
a

b

Fig. 4. Dependences of the calculated temperature on the x coordinate with the depth of the specimen as a parameter in 13 ns (*a*) and 30 ns (*b*) from the beginning of the annealing: *1* – 38 nm, *2* – 100 nm, *3* – 200 nm, *4* – 300 nm, *5* – 400 nm. Laser pulse intensity is 52 MW/cm^2

Fig. 5. Time dependences of the calculated temperature at different depths of the specimen at the center of the laser beam: *1* – 0 nm, *2* – 18 nm, *3* – 38 nm, *4* – 80 nm, *5* – 138 nm. Laser pulse intensity is 52 MW/cm^2

Fig. 6. Calculated dependences of the temperature on the depth of the specimen at the center of the laser beam at different times: *1* – 1 ns, *2* – 10 ns, *3* – 20 ns, *4* – 30 ns, *5* – 80 ns. Laser pulse intensity is 52 MW/cm^2

of the specimen is heated. In 13 ns from the beginning of the annealing, the temperature on the specimen surface reaches its peak, but it is not enough to heat the specimen volume (Fig. 4, *a*). Due to the heat conduction, the temperature of the entire volume of the specimen increases, and, at the same time, the temperature in the region of the action of a laser beam is higher as compared to other parts of the specimen (Fig. 4, *b*).

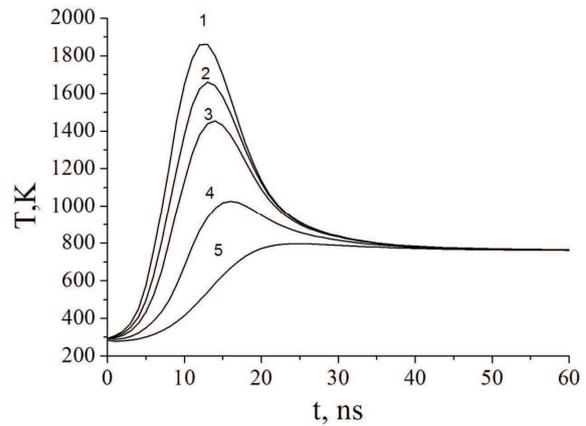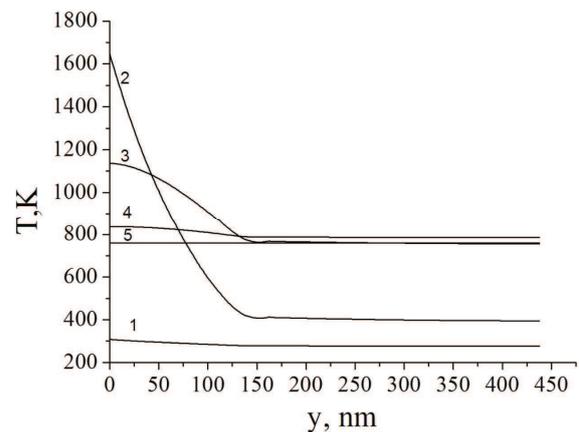The time dependences of the temperature distributions at the center of the laser beam at different depths are presented in Fig. 5. The plots show that the maximum temperature decreases, as the distance from the surface increases. But in 35 ns, the temperature at all points becomes the same and doesn't change, by indicating the establishment of a thermodynamic equilibrium. Figure 6 shows the temperature distributions over the depth of the specimen at different times. In the early stages of the annealing, there is a large temperature gradient over the thickness of the specimen. But already in 30 ns, the specimen is heated in the direction of the laser beam, and the temperature is stabilized.
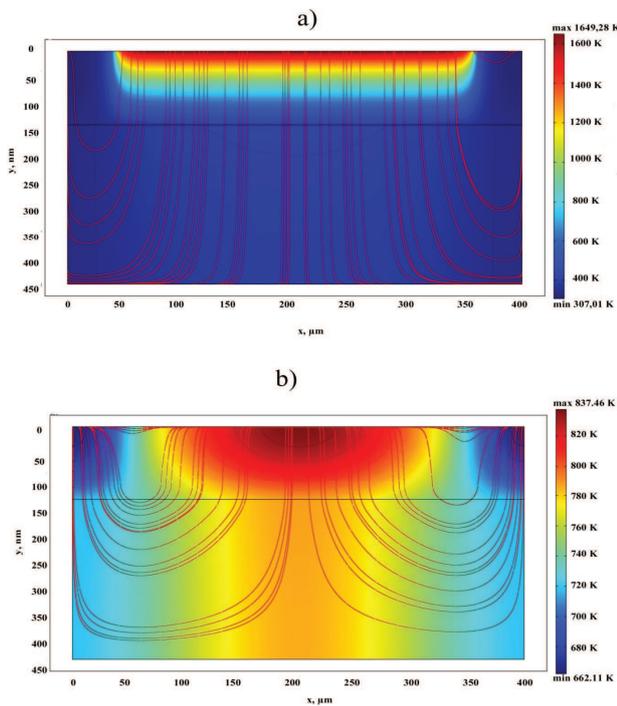
Fig. 7. Temperature profiles in the specimen in 10 ns (*a*) and 30 ns (*b*) from the beginning of the annealing with a laser intensity of 52 MW/cm^2. The lines are the heat flow directions

Figure 7 shows the temperature profile in the specimen at different times. As can be seen, the maximum temperature is concentrated after the laser pulse in the surface region of the SiO$_x$ film, and the heat flow is mainly directed into the depth of the specimen. The film volume is barely warmed, and the silicon substrate remains at the initial temperature. In 30 ns from the beginning of the annealing (Fig. 7, *b*), the SiO$_x$ film and the silicon substrate are heated, and the maximum temperature is decreased due to the heat outflow from the film surface and to the bottom of the substrate, as indicated by the direction of the heat flux lines. Note that there is no heat flow from side edges, because, according to our model, the condition of insulation is imposed for the specimen sides.

4. Conclusion

The laser annealing can be used for the formation of Si nanocrystals in a nonstoichiometric SiO$_x$

film. Such annealing allows localizing the treatment process of a specimen without destroying other items that are located on the same substrate with the film. The difficulties that arise in the simulation of the temperature distribution in the film and the formation of silicon nanocrystals with the predicted number and density at various depths of the specimen are caused by the fact that, during the laser annealing, the temperature on the surface and in the bulk are unevenly distributed. Therefore, the laser annealing of SiO$_x$ films requires further study.

As a result of the theoretical modeling of laser annealing of the nonstoichiometric SiO$_x$ films, it has been shown that the temperature on the surface can reach 1800 K. The temperatures of the specimen at higher intensities of laser irradiation are enough to stimulate the phase transition of the SiO$_x$ film into a nanocomposite SiO$_2$(Si) film with Si nanocrystals. The specimen volume is heated as a result of the heat conduction after the laser annealing, but the temperature in the area of a laser beam is higher as compared to other parts of the specimen. This allows us to predict the region of the formation of silicon nanoparticles.

1. S.V. Bunak, A.A. Buyanin, V.V. Ilchenko, V.V. Marin, V.P. Melnik, I.M. Khacevich, O.V. Tretyak, and A.G. Shkavro, Semicond. Phys., Quantum Electr. & Optoelectr. **13**, 12 (2010).

2. O.L. Bratus', A.A. Evtukh, O.S. Lytvyn, M.V. Voitovych, and V.O. Yukhymchuk, Semicond. Phys., Quantum Electr. & Optoelectr. **14**, 247 (2011).

3. I.Z. Indutnyi, E.V. Michailovska, P.E. Shepeliavyi, and V.A. Dan'ko, Semiconductors **44**, 218 (2010).

4. T. Inokuma, Y. Wakayama, T. Muramoto, R. Aoki, Y. Kurata, and S. Hasegawa, J. Appl. Phys. **83**, 2228 (1998).

5. C-J. Lin, G-R. Lin, Y-L. Chueh, and L-J. Chou, Electroch. and Solid-State Lett. **8**, No. 12, 43 (2005).

6. N.I. Koroteev and I.L. Shumay, *Physics of Power Laser Irradiation* (Nauka, Moscow, 1991) (in Russian).

7. A.V. Lykov, *The Theory of Heat Conduction* (Vysshaya Shkola, Moscow, 1967) (in Russian).

8. H.S. Carslaw and J.C. Jaeger, *Conduction of Heat in Solids* (Oxford Univ. Press, New York, 1959).

9. O.O. Gavrylyuk and O.Yu. Semchuk, Optoelectr. Information-Power Techn. **2**(24), 127 (2012).

10. D. Burgess , P.C. Stair, and E. Weitz, J. Vac. Sci. Technol. **4**, 1352 (1986).

11. E. Armon, Y. Zving, G. Laufer, and A. Soldan, J. Appl. Phys. **65**, 4995 (1989).

12. T. Rantala and J. Levoska, J. Appl. Phys. **65**, 4475 (1989).

13. G.A. Korn and T.M. Korn, *Mathematical Handbook for Scientists and Engineers* (McGraw-Hill, New York, 1961).

14. O.Yu. Semchuk, V.N.Semioshko, L.G. Grechko, M. Willander, and M.Karlsteen, Appl. Surf. Sci. **252**, 4759 (2006).

15. O.O. Gavrylyuk and O.Yu. Semchuk, Chem., Phys. and Techn. of Surface **3**, 352 (2012).

16. O.O, Gavrylyuk, O.Yu. Semchyk, O.L. Bratus, A.A. Evtukh, O.V. Steblova, and L.L. Fedorenko, App. Surf. Sci. 10.1016/j.apsusc.2013.09.171 (2013).

17. G.A. Kachurin, A.F. Layer, K.S. Zhuravlyov, I.E. Tyschenko, A.K. Gutakovskiy, V.A. Volodin, V. Scorupa, and R.A. Yankov, Fiz. Tekhn. Poluprov. **32**, 1371 (1998).

18. C.F. Tan, X.Y. Chen, Y.F. Lu, Y.H. Wu, B.J. Cho, and J.N. Zeng, J. Laser Appl. **16**, 40 (2004).

О.О. Гаврилюк, О.Ю. Семчук,
О.В. Стеблова, А.А. Євтух, Л.Л. Федоренко

ДОСЛІДЖЕННЯ
РОЗПОВСЮДЖЕННЯ ТЕМПЕРАТУРНИХ
ПРОФІЛІВ В НЕСТЕХІОМЕТРИЧНИХ
ПЛІВКАХ SiO$_x$ ПРИ ЛАЗЕРНОМУ ВІДПАЛІ

Р е з ю м е

Проведено теоретичне дослідження розповсюдження температурних профілів в нестехіометричних плівках SiO$_x$ при лазерному відпалі одиничним імпульсом. Розраховано розподіл температури на поверхні плівок SiO$_x$, опромінених лазерним променем з різною інтенсивністю. Знайдено розподіл температури на різній глибині плівок SiO$_x$, опромінених лазерним променем з інтенсивністю 52 МВт/см^2. Показано, що при лазерному відпалі з інтенсивністю 52 МВт/см^2 температура на поверхні плівок SiO$_x$ може досягати 1800 K.